Abdominal Radiology (2021) 46:1062–1081
https://doi.org/10.1007/s00261-020-02752-8

REVIEW

Diagnostic approach to primary retroperitoneal pathologies: what the radiologist needs to know

Ferenc Czeyda-Pommersheim[1] · Christine Menias[2] · Annemarie Boustani[1] · Margarita Revzin[1]

Received: 26 May 2020 / Revised: 30 August 2020 / Accepted: 3 September 2020 / Published online: 17 September 2020
© Springer Science+Business Media, LLC, part of Springer Nature 2020

Abstract

Retroperitoneal soft tissue lesions represent a wide range of disease processes with overlapping imaging findings. Familiarity with the CT and MR characteristics of these conditions is important to guide clinical evaluation. We review the tissue types, characteristic clinical, demographic, and imaging features of retroperitoneal tumors and tumor-like non-neoplastic conditions with CT and MR correlation, including anatomic and imaging clues, and provide a diagnostic approach to aide the radiologist in making a specific diagnosis.

Keywords Retroperitoneum · Mesenchymal tumors · Neurogenic tumors · Amyloidosis · Erdheim–Chester disease · Arteriovenous malformation

Introduction

A wide range of benign and malignant pathologies arise from the retroperitoneal spaces of the abdomen and pelvis. In general, a mass or process is considered to be primary to the retroperitoneum if it originates from the soft tissues, lymphatics or neural tissue of the retroperitoneum and not from its solid organs. This heterogeneous group of diseases often poses a diagnostic challenge for radiologists.

Two Main categories of primary retroperitoneal pathologies are recognized: neoplastic and non-Neoplastic. The majority of primary retroperitoneal neoplasms are malignant (Table 1) [1–4]. Although a definitive diagnosis often cannot be established on imaging, the primary role of the radiologist is to determine whether a biopsy is necessary and/or if the mass is resectable.

Primary retroperitoneal non-neoplastic pathologies include Castleman disease, extramedullary erythropoiesis Erdheim–Chester disease and amyloidosis many of which demonstrate characteristic imaging findings that are important to recognize in order to avoid unnecessary biopsy or surgery (Table 2).

In this article, we review neoplastic and non-neoplastic primary retroperitoneal conditions, their relevant pathophysiology, clinical presentation, and characteristic CT and MRI imaging findings, particularly key features that can aid in establishing an accurate diagnosis and guide therapy. Additionally, we will provide a comprehensive diagnostic approach for the differentiation of neoplastic from non-neoplastic pathologies that can serve as a road map for narrowing the differential diagnosis and allow for appropriate and timely management.

Anatomy of the retroperitoneum at a glance

A comprehensive knowledge of retroperitoneal anatomy is invaluable to accurately characterize and diagnose its conditions. The retroperitoneum can be grossly divided into several spaces: the anterior and posterior pararenal spaces, the perirenal space, and the fat-containing great vessel space. These can be further divided by separating the anterior pararenal space into the pancreatoduodenal space (containing the pancreas and duodenum) and the pericolonic space

CME activity This article has been selected as the CME activity for the current month. Please visit https://ce.mayo.edu/node/103122 and follow the instructions to complete this CME activity.

✉ Ferenc Czeyda-Pommersheim
Ferenc.Czeyda-Pommersheim@yale.edu

[1] Department of Radiology and Biomedical Imaging, Yale School of Medicine, 333 Cedar Street, PO Box 208042, New Haven, CT 06520, USA

[2] Department of Radiology, Mayo Clinic, Phoenix, AZ, USA

Table 1 Imaging, clinical features and differential considerations of retroperitoneal neoplasms

Tumors of soft tissue origin			
Liposarcoma: well differentiated or dedifferentiated (low to intermediate grade)	Demographics: middle aged and older Clinical: Asymptomatic until large enough to produce mass effect	Mixed fat and soft tissue density	Lipoma: entirely composed of fat, imaging cannot distinguish Myelolipoma: centered in the adrenal gland PEComa: gross fat-containing soft tissue mass often in women with tuberous sclerosis
Liposarcoma: myxoid (high grade)	Demographics: middle-aged adults	Soft tissue mass with cystic/fluid signal components, irregular ill-defined	Necrotic tumor (e.g., leiomyosarcoma or rhabdomyosarcoma) Abscess: clinical history
Leiomyosarcoma	Demographics: middle aged to older Clinical: Asymptomatic unless from mass effect	Soft tissue mass closely associated with/extending into the IVC Hypovascular, central necrosis common Significant local adenopathy is uncommon	Angiosarcoma: significant local adenopathy is common UPS : not associated with IVC
Undifferentiated pleomorphic sarcoma (UPS)	Demographics: middle aged and older Pathology: fibroblasts and myofibroblasts	Soft tissue mass with calcification Arterial enhancement and delayed hypoenhancement	Granulomatous infection: clinical/laboratory evidence of infection Treated lymphoma: clinical history
Rhabdomyosarcoma	Demographics: most common in children Clinical: asymptomatic unless from mass effect	Soft tissue mass with large necrotic areas	Myxoid liposarcoma: fluid-appearing components often at least partially enhance Abscess: enhancing soft tissue component is comparatively small, clinical history
Angiosarcoma	Demographics: older adults Pathology: vascular endothelial origin Clinical: usually occur in the skin, rarely in the retroperitoneum	Prominent internal neovascularity Local adenopathy is common	Similar to other aggressive retroperitoneal malignancies
Chondrosarcoma	Demographics: middle-aged adults Clinical: retroperitoneal primary is very rare compared to skeletal origin tumors	Stippled, arc-like internal calcification	Similar to other aggressive retroperitoneal malignancies
Synovial sarcoma	Demographics: middle-aged adults	Heterogenous mass with hemorrhage, necrosis and calcification	UPS/Myxoid liposarcoma/Rhabdomyosarcoma: may be indistinguishable on imaging
Peripheral epithelioid tumor (PEComa)	Pathology: epithelioid and spindle cells arranged around blood vessels; may be benign or malignant Clinical: associated with tuberous sclerosis	Large infiltrative heterogenous soft tissue mass May have gross internal fat or large necrotic components	Similar to other aggressive retroperitoneal malignancies
Desmoid tumor	Demographics: young to middle-aged adults, F > M Pathology/lab: benign appearing monoclonal spindle cells Clinical: patients often have prior history of surgery or trauma, associated with familial adenomatous polyposis	Homogenous CT and MRI signal very similar to muscle Marked T2 hypointensity	Lymphoma: associated with diffuse lymphadenopathy Carcinoid mesenteric root metastasis: carcinoid typically enhances in the arterial phase, has pancreas or small bowel primary Surgical or traumatic scar: non mass-like

Table 1 (continued)

Neurogenic tumors			
Schwannoma	Demographics: F > M, young to middle age (30-60 yo) Pathology: nerve sheath origin Clinical: pain associated with movement, paresthesia, weakness	Heterogenous in texture, may be hemorrhagic Extend along the nerve-entering exiting nerve sign Fascicular sign-aka fascilular bundles; encapsulated, contains myxoid stroma	Neurofibroma- more often fusiform, "target" sign is more common, hemorrhage Neuroblastic tumor-pediatric patient, intraspinal extension through neural foramen ("dumbbell" tumor)
Neurofibroma	Demographics: M > F, Localized form: young to middle aged, associated with NF1 Diffuse form: children to adults Pathology: nerve sheath origin, can malignantly transform, especially plexiform NF Clinical Sx: in localized form may be asymptomatic, symptoms vary based on compression of adjacent structures	May have a targetoid appearance on CT and MRI expansion of the entire nerve, with nerve fibers coursing through the mass itself; dumbbell shape if extend via neural foramen, contains myxoid stroma	Schwannoma: difficult to distinguish from NF, more common hemorrhage and cystic/fatty degeneration, target sign is less common; eccentrically located tumor may be separated from nerve Malignant peripheral: NST more likely has hemorrhage and necrosis, locally invades, larger size, more often peripheral enhancement, intratumoral cysts
Ganglioneuroma	Demographics: young, M = F Pathology: originates from sympathetic ganglia	Heterogenous soft tissue elongated shape mass along sympathetic chain Extend into spaces between structures and surround vessels without compression May contain punctate calcifications May contain myxoid stroma May contain hemorrhage	Teratoma: fat and Ca++ in multilocular cystic lesion Neurogenic neoplasm: spherical lesions centered on neural foramen Ganglioneuroblastoma: - children < 10yo, presence of metastases to liver, lymph nodes, lung
Paraganglioma	Demographics: young, M = F, associated with VHL, NF1, MEN syndromes Pathology/lab: originated from chromaffin cells, may be malignant Clinical: May be symptomatic from catecholamine secretion	Large heterogenous elongated mass May contain hemorrhage/calcification, hypervascular, draining veins Octretotide scan diagnostic	Metastases: evidence of primary elsewhere Schwannoma: rare hemorrhage and no dilated vessels (flow voids on MRI)
Germ cell tumors			
Primary extragonadal germ cell tumor	Demographics: M > F Pathology/lab: originates from aberrant primordial germ cell rests; AFP and Hcg may be elevated	Solid heterogenous mass Seminomas: microcalcifications Non-seminomatous tumors: heterogenous with hemorrhage	Metastatic disease: evidence of a primary elsewhere Lymphoma: usually more homogenous and associated with diffuse adenopathy, calcifications rare
Primary sex cord stromal tumors	Pathology/lab: originates from sex cord stromal tissue or sex cord-like differentiation of somatic cells Estrogen levels may be elevated	Solid heterogenous mass	Metastatic disease: evidence of a primary elsewhere Lymphoma: usually more homogenous and associated with diffuse adenopathy
Teratoma	Demographics: bimodal age distribution, F > M Pathology/lab: pluripotent stem cell origin, AFP may be elevated	Mature: large cystic components, may contain fluid/fluid levels, calcium or fat Immature: Smaller cysts, small foci of fat or calcium, invasive mass	Liposarcoma: may not be possible to distinguish on imaging

(surrounding the ascending and descending colon). Below the level of the kidneys, the anterior and posterior pararenal spaces merge to form an infrarenal retroperitoneal space, which in turn communicates inferiorly with the prevesical space and extraperitoneal compartments of the pelvis (Fig. 1) [5]. Several signs can be used to differentiate peritoneal from retroperitoneal masses, via determination of the organ of tumor origin (Table 3) [6].

Diagnostic imaging approach to differentiate neoplastic from non-neoplastic pathologies and suggested management

Imaging plays a major role in the detection and characterization of retroperitoneal pathologies, and recognition of key imaging features can help in narrowing the differential diagnosis. Both contrast-enhanced CT and MRI are useful for tissue characterization, accurate determination of mass origin and extent, and assessment of benign or malignant potential.

Morphology is an important clue as to whether a retroperitoneal soft tissue mass is malignant. On imaging, benign processes often have a non-mass-like appearance surrounding and encasing adjacent anatomical structures, such as mantle-like encasement of the ureters and vessels with tethering and luminal narrowing. Inflammatory processes may cause wall thickening and pseudoaneurysm formation of the aorta or mesenteric arteries. Malignant tumors present with more well-defined borders and mass-like appearances and are commonly associated with adjacent organ and/or structure displacement/distortion.

A mass centered in the retroperitoneum often indicates malignancy. For most primary retroperitoneal malignancies, the only curative treatment is complete resection with a tumor-free margin. Therefore, when a diagnosis of primary malignancy is likely, patients usually are referred for surgical evaluation.

In contrast, chemotherapy is usually the first line treatment for lymphoma and metastatic disease. When these entities are considered on imaging (specifically when a primary neoplasm is detected elsewhere), biopsy should be suggested for confirmation (also see Table 4). Individual conditions, grouped by tissue type, will be discussed in greater detail in the subsequent section.

Imaging findings that suggest a specific primary retroperitoneal malignancy: resection should be considered

Fat components

The presence of gross fat in a primary retroperitoneal mass that also has myxoid, solid, infiltrative or nodular soft tissue components strongly suggests liposarcoma (Fig. 2). Tumors not primary to the retroperitoneum, such as adrenal myelolipoma or renal angiomyolipoma, also contain gross fat intermixed with soft tissue; however, these are centered or completely contained within their respective organs of origin (Fig. 3). Retroperitoneal lipomas appear as well-defined masses with homogenous fat attenuation. Although benign, lipomas cannot be distinguished from well-differentiated liposarcomas on imaging and any purely fatty mass should be treated as a liposarcoma until confirmed otherwise by histology [7]. Other primary retroperitoneal tumors to consider when gross fat is present include teratoma (usually demonstrates calcification and heterogeneous enhancement) and extra-adrenal myelolipoma (a rare entity, most commonly in the presacral space) [1, 8].

Intravascular extension

A primary retroperitoneal lesion with intravascular growth is characteristic of leiomyosarcoma (Fig. 4). The main differential consideration is intravascular spread of an abdominal or pelvic solid organ primary malignancy, most commonly hepatocellular carcinoma, adrenal cortical carcinoma, renal cell carcinoma, or uterine metastasizing leiomyoma. Therefore, evidence of a primary mass in any of these organs should be sought.

Myxoid stroma

Neurogenic tumors, myxoid liposarcomas, and myxofibrosarcomas are the most common retroperitoneal tumors that contain myxoid matrices, which on MRI has characteristic marked T2 hyperintensity as well as delayed contrast enhancement [2, 9]. Progressive enhancement peaking on the delayed phase distinguishes myxoid stroma from internal necrosis within a mass, which does not enhance.

Necrotic component

Necrosis is a characteristic finding of large or high-grade neoplasms. When necrosis is seen in retroperitoneal tumors leiomyosarcoma, undifferentiated pleomorphic sarcoma, PEComas, and pleomorphic liposarcomas are the main differential considerations. Necrotic tissue is heterogeneously

Table 2 Imaging, clinical features, and differential considerations of non-neoplastic primary retroperitoneal conditions

Non-neoplastic conditions			
Retroperitoneal hemorrhage	Demographics: variable Pathology: due to anticoagulation or injury	Ill-defined infiltration of the retroperitoneum with high CT attenuation and high T1 signal material on MRI in the acute phase. Hemosiderin in chronic hematoma markedly T2 hypointense Hematocrit level may be seen in loculated hematomas	Amyloidosis: infiltrating soft tissue is same CT density and T1 attenuation as muscle, may calcify if chronic
Arterialvenous malformation	Demographics: variable Pathology: congenital or acquired	Tangle of vessels with prominent flow voids in high flow lesions on MRI	Primary retroperitoneal sarcomas: tangle of vessels is uncommonly seen, large soft tissue component usually present in malignancy
Abscess	Demographics: variable Pathology: related to infection of adjacent abdominal/retroperitoneal organs	Fluid collection with enhancing wall	Necrotic mass: Malignancy has a large soft tissue component Myxoid tumors: Fluid-attenuation components show reticular enhancement in myxoid tumors
Erdheim–Chester disease	Demographics: middle aged, F = M Pathology/lab: non-Langerhans cell histiocytosis, multisystem disorder	Soft tissue encasing retroperitoneal organs and structures Bilateral symmetric osteosclerosis of the metaphyses and diaphyses of the long bones	Chronic periaortitis-may not be possible to distinguish on imaging Retroperitoneal fibrosis: in early phase may not be possible to distinguish. ECD does not displace/obstruct ureters or other structures
Retroperitoneal Fibrosis	Demographics: M > F, middle aged Pathology/lab: autoimmune process Clinical: back pain due to obstruction of ureters, aorta, IVC	Soft tissue encasing retroperitoneal structures Active phase: T2 hyperintense, chronic phase: T2 hypointense scar on MRI Benign: medial displacement of ureters Malignant form: lateral displacement of ureters	Chronic periaortitis-may not be possible to distinguish on imaging Metastases-more discrete and asymmetric, more heterogeneous and higher signal on T2WI, evidence of a primary mass Lymphoma-more cephalic location in retroperitoenum, no ureter obstruction, no mass effect on vessels
Extramedullary hematopoiesis	Pathology/lab: extramedullary deposition of hematopoietic elements. Clinical: abdominal pain, organomegaly, severe anemia	Soft tissue masses with heterogenous enhancement	Lymphoma-more cephalic location in retroperitoenum, no ureter obstruction, no mass effect on vessels Metastatic disease: evidence of a primary elsewhere
Castleman's disease	Demographics: across all ages, M = F, often in patients with HIV and Kaposi sarcoma Pathology/lab: Angiofollicular lymph node hyperplasia Clinical: asymptomatic or pain, anorexia, vomiting	Homogenous soft tissue masses, may have calcifications, associated lymphadenopathy	Lymphoma- confluent nodal or discrete visceral soft tissue mass with no calcifications, high FDG avidity on PET, marked diffusion restriction on MRI Neurogenic tumor well-circumscribed or infiltrative masses, w/wo Ca++

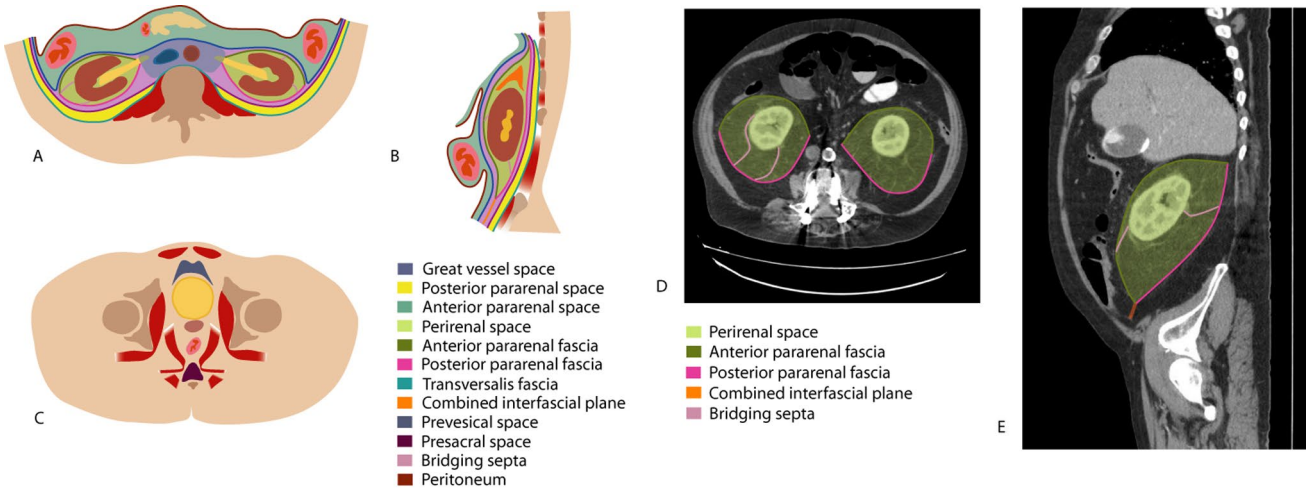

Fig. 1 Schematic diagram of retroperitoneal anatomy with CT correlation. The anterior pararenal space **a**, **b** is delineated by the peritoneum anteriorly and the anterior pararenal facia posteriorly and contains the pancreas and transverse colon. The posterior pararenal space (**a**, **b**), primarily composed of fat, is bounded by the posterior pararenal fascia anteriorly and the transversals fascia posteriorly. The great vessel space **a** contains the aorta, the inferior vena cava, fat, neural tissue, and lymphatics. Many of the retroperitoneal spaces are contiguous with extraperitoneal spaces of the pelvis (**c**). The perirenal space **b**, **d**, **e** is bounded by the anterior and posterior perirenal fasciae and contains fat as well as bridging septa that extend from the renal capsule to the perirenal fascia (**e**)

Table 3 Signs used to differentiate peritoneal from retroperitoneal masses via determination of the organ of tumor origin

Type of the sign	Description	Schematic diagram
The invisible organ sign	When a large mass arises from a small organ, the organ sometimes becomes undetectable aka obliterated by the tumor	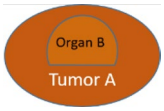
The embedded organ sign	A. When a tumor compresses an adjacent plastic organ (GI, IVC) that is not the organ of origin, the organ is deformed into a crescent shape. B. When tumor arises from an organ the organ appears to be embedded in the tumor	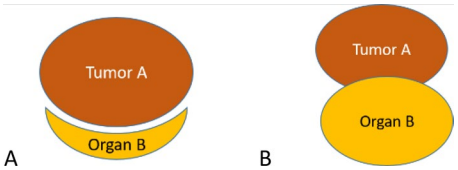
The beak sign	A. When a mass deforms the edge of an adjacent organ into a "beak" shape, it is likely that the mass arises from that organ B. When tumor does not arise from organ	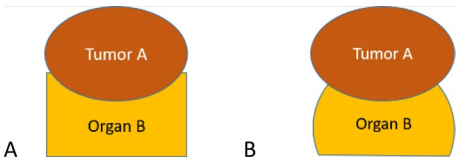

hyperintense on T2WI and demonstrates no enhancement on post-contrast imaging [6].

Hypervascularity

Among the hypervascular lesions are paragangliomas, leiomyosarcoma, myxofibrosarcoma, other sarcomas, and arteriovenous malformations and fistulas. Hypervascularity differentiates these from entities that are usually hypovascular such as lymphoma, multiple myeloma, and low-grade sarcomas [10]. Other imaging characteristics of these lesions that further narrow the differential will be subsequently discussed.

Imaging findings for which clinical management is uncertain: Surgery versus watchful waiting

Cystic contents

Many benign neoplasms have relatively large cystic components and may pose a diagnostic challenge. Examples of cystic masses include cystic lymphangiomas cystic

Table 4 Imaging findings of retroperitoneal pathologies grouped by clinical management recommendation

	Imaging finding	Primary diagnostic consideration	Differential considerations
Specific malignancy: resection should be considered	Mass with intermixed fat and soft tissue elements	Liposarcoma	Teratoma: calcifications are common Extra-adrenal myelolipoma: rare, usually in the presacral space Adrenal myelolipoma, renal AML: centered in their respective organs of origin Lipoma: entirely composed of fat, indistinguishable from low-grade liposarcoma on imaging
	Mass with direct extension into the IVC	Leiomyosarcoma	Abdominal or pelvic solid organ primary tumors (e.g., hepatocellular carcinoma, adrenal cortical carcinoma): mass is centered in their respective organ of origin
	Mass with myxoid components	Myxoid liposarcoma Myxofibrosarcoma	Neurogenic tumors: paravertebral location
	Mass with necrotic components	Leiomyosarcoma undifferentiated pleomorphic sarcoma PEComas	Tumor with myxoid components: internal liquid-appearing contents do not enhance in necrotic tumors
	Hypervascular mass	paragangliomas, leiomyosarcoma, myxofibrosarcoma	Hypervascular metastases: multiple masses, known primary tumor elsewhere
Favor benign: management uncertain	Large cystic components	Cystic lymphangioma Cystic mesothelioma Epidermoid cyst Cystic schwannoma/paraganglioma	Necrotic tumor: Large soft tissue component in addition to cystic component
Suspect malignancy: biopsy should be considered	Mass-like morphology	Primary or metastatic malignancy	Lymphoma: marked lymphadenopathy Metastatic disease: known primary elsewhere
	Lymphadenopathy	Lymphoma: marked adenopathy, "sandwich sign"	Metastatic disease: known primary elsewhere
Benign imaging characteristics	Benign morphology	Inflammatory processes (e.g., RPF) Amyloidosis Erdheim–Chester disease	Lymphoma: marked lymphadenopathy, splenomegaly, displaces but does not obstruct vasculature

mesotheliomas (rare benign neoplasms of mesothelial origin), ganglioneuromas, cystic schwannomas, paragangliomas, cystadenomas, and epidermoid cysts.

Imaging findings that are nonspecific but suggest malignancy: biopsy should be considered

Lymphoma and metastatic disease typically require tissue confirmation. Imaging findings indicative of either should prompt recommendation of biopsy.

Enlarged abdominopelvic lymph nodes can indicate lymphoma or metastatic disease. Lymphoma usually produces nodes in multiple contiguous anatomic distributions. The nodes are homogenous, mildly enhancing, and surround but not occlude the vasculature. Splenomegaly with or without splenic nodules may be present. Metastatic adenopathy is typically heterogeneous. Necrosis may be present if the nodes are large and they may obstruct vasculature, bowel, or the ureters. When metastatic disease is suspected, parenchymal organs should be closely examined for evidence of a primary mass or other metastases.

Differential considerations of malignant retroperitoneal tumors based on tissue type

Primary retroperitoneal lesions with characteristics of a mass are often malignant [1–4]. These lesions are typically asymptomatic until they become large and come to clinical attention when symptoms develop from mass effect. With

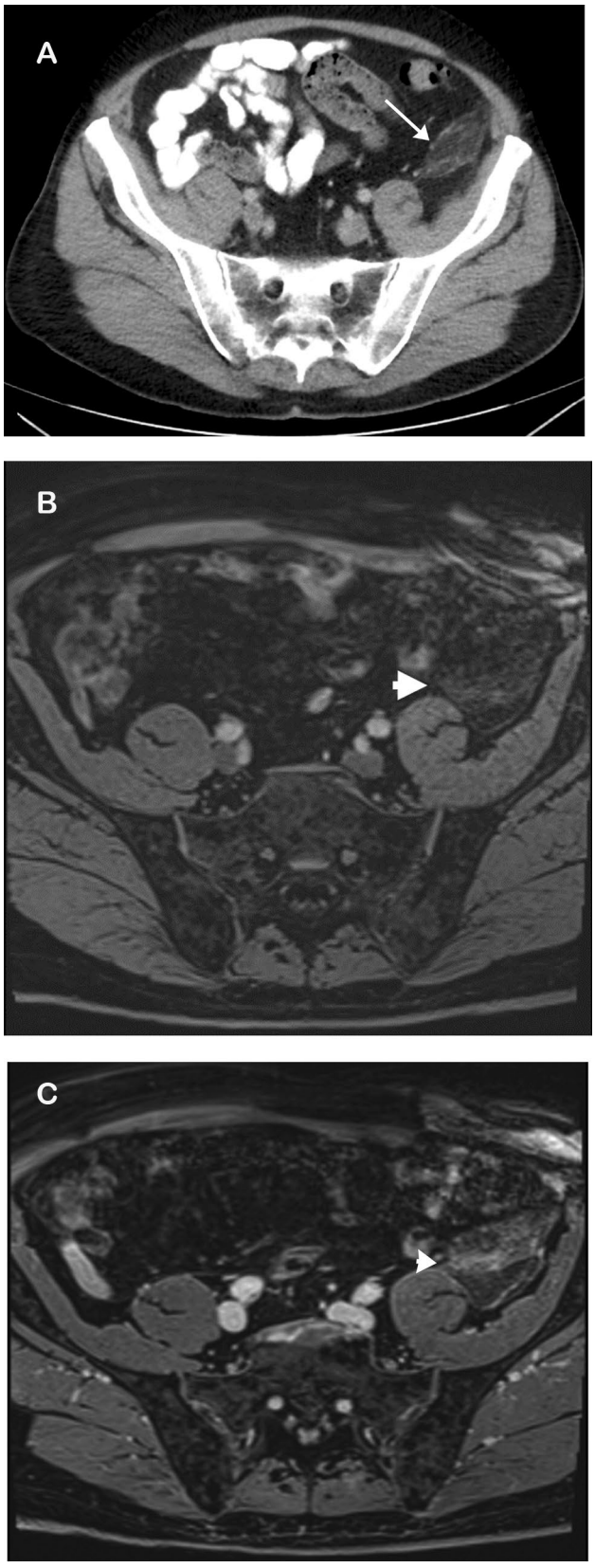

Fig. 2 **a** Liposarcoma in a middle-aged man. **a** Contrast-enhanced ▶ CT shows a mixed fat and soft tissue attenuation mass in the pelvis (arrow). **b** Axial T1W FS post-contrast MRI shows enhancement of the soft tissue components of the mass (arrowhead). **b** Liposarcoma in a middle-aged man. **a** Contrast-enhanced CT shows a mixed fat and soft tissue attenuation mass in the pelvis (arrow). **b/c** Axial T1W FS pre- (**b**) and post-contrast **c** MRI shows enhancement of the soft tissue components of the mass (arrowhead). **c** Liposarcoma in a middle-aged man. **a** Contrast-enhanced CT shows a mixed fat and soft tissue attenuation mass in the pelvis (arrow). **b/c** Axial T1W FS pre- (**b**) and post-contrast (**c**) MRI shows enhancement of the soft tissue components of the mass (arrowhead)

the exception of a few select tumor types that are discussed below, there are no laboratory or clinical abnormalities that suggest a specific tumor. For clinical and demographic characteristics of these conditions please refer to Table 1.

Primary retroperitoneal neoplasms

Mesenchymal tumors

Liposarcoma Liposarcomas are most common primary tumors to arise in the retroperitoneum [11–13]. The only potentially curative treatment is resection with a tumor-free margin. Local or regional recurrence is the most common cause of death. Distant metastases are most often to the lungs [14].

Liposarcomas are divided into 5 histologic subtypes: well differentiated, dedifferentiated, myxoid, pleomorphic and not otherwise specified [15]; of these differentiated/dedifferentiated liposarcomas are the most common [16]. More than one histologic subtype can co-exist within the same tumor, in these cases, overall prognosis depends on the least differentiated subtype.

Imaging has a critical role both in diagnosis and staging. Most liposarcomas present as large well-defined masses of mixed fluid and soft tissue components that avidly enhance with intravenous contrast (Fig. 2). Gross fat is not always present, but when found in a heterogeneous retroperitoneal mass not arising from a solid organ strongly suggests liposarcoma. Differential considerations for a gross fat-containing retroperitoneal mass include lipomas, which are homogenous and entirely composed of fat with no soft tissue components, and PEComas, which have a dominant soft tissue component but may contain smaller amounts of gross fat.

The imaging appearance of liposarcomas correlates with their histologic composition [17]. A higher ratio of soft tissue compared to lipid is found in high-grade tumors [18, 19]. Well-differentiated liposarcomas typically present as well-circumscribed masses nearly completely composed of gross fat, with a small nodular, reticular, or hazy soft tissue component (Fig. 2). Dedifferentiated liposarcomas, considered intermediate grade, contain a larger proportion

of internal nonlipid soft tissue [20]. Myxoid components in liposarcomas are indicative of higher grade and can be readily distinguishable on imaging, as the myxoid components are similar to fluid on non-contrast CT and show T2 hyperintense signal when compared to muscle on MRI. On post-contrast imaging, unlike fluid-containing structures, myxoid tumors show gradual reticular internal enhancement (Fig. 3) [15, 19].

Leiomyosarcoma Leiomyosarcomas are mesenchymal tumors that show smooth muscle differentiation. The retroperitoneum is the most common site of origin of leiomyosarcomas. Treatment is surgical. Retroperitoneal leiomyosarcomas are classified into IVC and non-IVC origin tumors; although the two subtypes are resected through a different surgical approach, they are similar in their internal composition, metastatic pattern and long-term prognosis [21].

The majority of non-IVC origin leiomyosarcomas arise in the perirenal space of the retroperitoneum. Tumors that originate from the IVC wall and most commonly arise at or caudal to the level of the retrohepatic IVC, presenting at an earlier stage due to development of clinical symptoms related to IVC obstruction. Metastases are typically hematogenous, most commonly to the lungs, liver, bone, soft tissue and the peritoneum [22]. Local lymph node metastases are uncommon. This distinguishes leiomyosarcomas from angiosarcomas which also present as a soft tissue mass arising from the IVC but more commonly metastasize to local lymph node chains [23].

On imaging, leiomyosarcomas present as a large, heterogeneous, infiltrative, lipid-free soft tissue mass, similar to muscle on CT and T1WI, hyperintense to muscle on T2WI with heterogeneous enhancement. A central necrotic or avascular area is also often present [24, 25]. Although most leiomyosarcomas are extraluminal, if a mass is centered within the IVC lumen, it can be confidently diagnosed as a leiomyosarcoma of IVC origin (Fig. 4) [26]. The vessel lumen may be partially or completely occluded and is often expanded [24].

Undifferentiated pleomorphic sarcoma (UPS) Undifferentiated pleomorphic sarcomas (UPS), previously called malignant fibrous histiocytomas, are tumors of mesenchymal origin composed of fibroblastic or myofibroblastic cells. UPS is the third most common type of primary malignancy in the retroperitoneum, following liposarcoma and leiomyosarcoma [4, 27]. Treatment is surgical.

On imaging, UPS present as large heterogeneous tumors with similar signal characteristics to muscle except for hyperintense signal on T2WI, strong arterial enhancement and delayed hypoenhancement [28]. Although less common than in leiomyosarcomas, central necrosis may occur in large tumors (Fig. 5). Approximately 20% of UPS show internal calcification, which is uncommon in leiomyosarcomas [29, 30].

Similar to other soft tissue malignancies, including liposarcoma and leiomyosarcoma, UPS show diffusion restriction on MRI. Although diffusion restriction is useful to distinguish retroperitoneal malignancy from benign entities, its use in determining the specific type of malignancy is limited [31].

Less common sarcomas Other rare histologic subtypes of retroperitoneal sarcomas include rhabdomyosarcoma, angiosarcoma, chondrosarcoma, and synovial sarcoma. These tumors appear similar on imaging: a large soft tissue mass, heterogenous but similar to muscle in CT attenuation, primarily isointense to muscle on T1WI hyperintense on T2WI, with heterogenous enhancement. A few imaging characteristics that may help suggest a specific diagnosis include high flow vessels that show prominent T2 signal void within angiosarcomas, chondroid matrix with stippled, punctate and arc-like calcifications occasionally present in chondrosarcomas, and a prominent component of hemorrhage, necrosis, and calcification in synovial sarcomas [32–35].

Perivascular epithelioid cell tumor (PEComa) PEComas are mesenchymal neoplasms composed of epithelioid and spin-

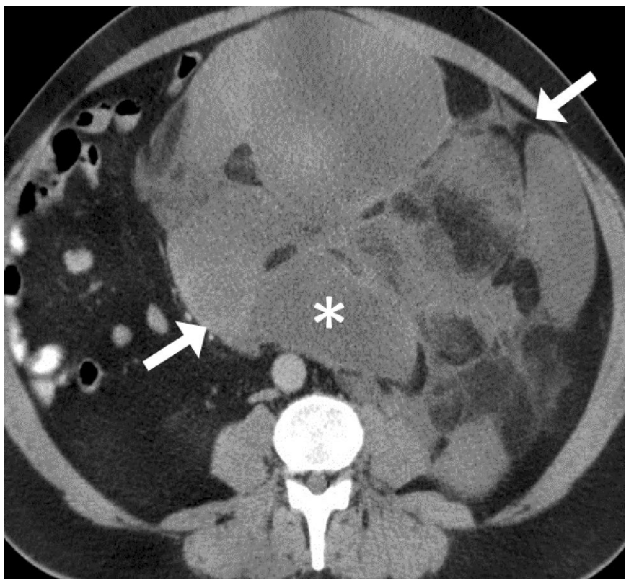

Fig. 3 Myxoid liposarcoma. Contrast-enhanced CT in the portal venous phase shows a mass (arrows) with mixed fat and soft tissue attenuation, including several fluid attenuating components (asterisk) corresponding to the myxoid components within a liposarcoma

dle cells arranged around blood vessels. Most PEComas are benign (such as angiomyolipoma and lymphangioleiomyomatosis), a minority of PEComas are malignant sarcomas that may arise in the retroperitoneum [36]. These tumors are associated with tuberous sclerosis, and have a female predominance and a poor prognosis [37]. Treatment is surgical.

PEComas do not have pathognomonic imaging findings and therefore tissue sampling is usually necessary for diagnosis. On imaging, retroperitoneal PEComas are large (> 5 cm) infiltrative heterogeneous masses that demonstrate avid arterial enhancement, areas of necrosis, hemorrhage, and occasional punctate foci of calcification [38]. Gross fat may be present, which can make these neoplasms indistinguishable from liposarcomas. Invasion of retroperitoneal organs may also be seen [39].

Lymphoma Most lymphomas involving the retroperitoneum originate from the urinary tract; a minority are of primary retroperitoneal origin. Treatment is chemotherapy. Characteristic imaging findings include well-circumscribed nodular or lobulated soft tissue masses of homogenous CT attenuation, T1WI hypointense and T2WI hyperintense signal and homogenous enhancement that peaks in the delayed phase. Involved retroperitoneal lymph nodes typically form a confluent lobulated soft tissue mass that extends into the pelvis or the mesentery (Fig. 6, Video 1). Lymphoma-related adenopathy tends to insinuate between rather than narrow adjacent vascular structures ("sandwich sign") [40, 41]. Necrosis, calcification, and hemorrhage are rare (Figs. 7, 8, 9, 10, 11, 12).

The primary differential diagnosis for infiltrative, confluent retroperitoneal soft tissue is retroperitoneal fibrosis (RPF). Both RPF and lymphoma have a similar imaging appearance, and therefore these entities may be indistinguishable on imaging. Extension of a mass beyond the retroperitoneum favors a diagnosis of lymphoma, as such extension is not typical for RPF. Anterior displacement of the aorta by a confluent nodal mass is more characteristic of lymphoma rather than RPF, which usually encases the vasculature without displacing it (Fig. 13). Diffusion restriction on MRI is more pronounced in lymphoma compared to RPF [41].

Neurogenic tumors Neurogenic tumors constitute 10–20% of all primary retroperitoneal malignancies. They are more likely to be benign and have a better prognosis. [42] In the retroperitoneum, they follow the distribution of the sympathetic ganglia and paraspinal areas, including the organs of Zuckerkandl. The main subcategories of neurogenic tumors in adults include nerve sheath tumors (schwannoma, neurofibroma), ganglionic cell tumors (ganglioneuroma), and paraganglionic cell tumors (paraganglioma).

Fig. 4 **a** Leiomyosarcoma in a middle-aged woman, endovascular growth. Contrast-enhanced CT in the portal venous phase shows a heterogeneous soft tissue mass completely filling and expanding the infrahepatic (arrow in **b**) and intra-hepatic (arrowheads in **a**) segments of the IVC. **b** Leiomyosarcoma in a middle-aged woman, endovascular growth. Contrast-enhanced CT in the portal venous phase shows a heterogeneous soft tissue mass completely filling and expanding the infrahepatic (arrow in **b**) and intra-hepatic (arrowheads in **a**) segments of the IVC

Neurofibroma and Schwannoma Neurofibroma (NF) and schwannoma are benign nerve sheath tumors. [43] NFs can be isolated (90%) or can occur in association with type 1 neurofibromatosis (NF1). On imaging, both tumors have a

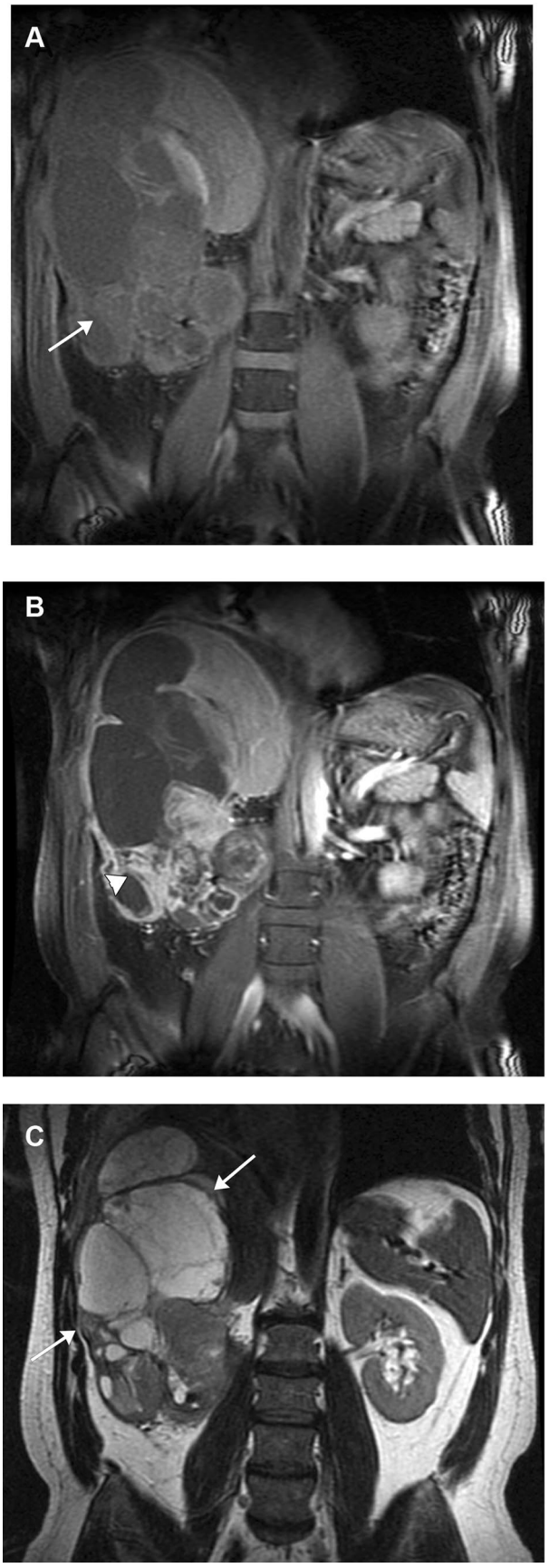

Fig. 5 A Undifferentiated pleomorphic sarcoma (formerly malignant ▶ fibrous histiocytoma) in a middle-aged man. **a** coronal T1W FS pre-contrast, **b** T1W FS post-contrast, **c** T2 TSE coronal images of the abdomen. T1 hyperintense signal within the mass is consistent with hemorrhage (arrow in **a**) and the mass also demonstrates heterogeneous enhancement (arrowhead in **b**). The T2W TSE image shows anatomic relationships of the mass (arrows in **c**) centered in the retroperitoneum. **b** Undifferentiated pleomorphic sarcoma (formerly malignant fibrous histiocytoma) in a middle-aged man. **a** coronal T1W FS pre-contrast **b** T1W FS post-contrast C: T2 TSE coronal images of the abdomen. T1 hyperintense signal within the mass is consistent with hemorrhage (arrow in **a**) and the mass also demonstrates heterogeneous enhancement (arrowhead in **b**). The T2W TSE image shows anatomic relationships of the mass (arrows in **c**) centered in the retroperitoneum. **c** Undifferentiated pleomorphic sarcoma (formerly malignant fibrous histiocytoma) in a middle-aged man. **a** coronal T1W FS pre-contrast, **b** T1W FS post-contrast, **c** T2 TSE coronal images of the abdomen. T1 hyperintense signal within the mass is consistent with hemorrhage (arrow in **a**) and the mass also demonstrates heterogeneous enhancement (arrowhead in **b**). The T2W TSE image shows anatomic relationships of the mass (arrows in **c**) centered in the retroperitoneum

variable appearance, demonstrating solid and/or cystic components depending on the degree of degeneration within the tumor, with possible hemorrhage and calcification. Due to the presence of myxoid degeneration, these tumors tend to be centrally hyperintense on T1WI, peripherally hyperintense on T2WI, and hypoattenuating on CT. On post-contrast imaging, homogeneous or target-like enhancement can be seen. NFs are unencapsulated and result in expansion of the entire nerve, with nerve fibers coursing through the mass itself. Plexiform neurofibromas have an infiltrative appearance with multiple sites of disease that track along nerve roots (Fig. 8). Malignant transformation is more common with neurofibromas. Schwannomas are encapsulated and usually extend along the course of a nerve, resulting in nerve flattening. The entering and exiting nerve signs may be apparent. Highly cellular components demonstrate hypointense signal on both T1 and T2WI (Fig. 7) [43, 44].

Ganglioneuroma Ganglioneuromas are benign tumors that arise from sympathetic ganglia and are most commonly located in the retroperitoneum, extending along the paravertebral sympathetic ganglia and sometimes the adrenal medulla. They carry a favorable prognosis. These tumors are most commonly asymptomatic, however, on occasion secrete catecholamines or androgenic hormones [45]. On imaging, ganglioneuromas are hypoattenuating masses that demonstrate hypointense T1 and hyperintense T2 signal, and occasionally present with a centrally located intact vessel (Fig. 9). Punctate calcifications are characteristic and seen in 20-30% of tumors [46]. Post-contrast enhancement is variable.

Paraganglioma (extra-adrenal pheochromocytoma) Paragangliomas are tumors related to chromaffin cells that

Fig. 6 Lymphoma in a 40-year-old man. Contrast-enhanced CT shows confluent mass-like lymphadenopathy in the retroperitoneum (black arrow) showing homogenous low-level enhancement with lymphadenopathy also extending to the root of the mesentery (arrowhead). The nodes displace and surround in spite of the degree of adenopathy do not obstruct the vasculature (arrow). A nodal mass surrounding the vasculature has been described as the "sandwich sign"

originate in an extra-adrenal location; most commonly in the organ of Zuckerkandl. Production/secretion of catecholamines and associated symptoms is a hallmark of these tumors, present in approximately 40% of cases [45]. They typically appear as a large mass with areas of hemorrhage and necrosis on cross-sectional imaging (Video 2). Large paragangliomas can be complicated by extensive retroperitoneal hemorrhage and rupture. Punctate calcifications and avid contrast enhancement are common. Metastases are seen in up to 50% of cases. [42]

Germ cell origin tumors (GCT) *Primary extragonadal GCT and sex cord stromal tumors* (*SCST*) Primary extragonadal GCT (Video 3) are thought to arise from aberrant primordial germ cell rests, and account for approximately 1–2.5% of all germ cell tumors [47]. Although the retroperitoneum is the second most common site of presentation, the majority of retroperitoneal GCTs represent metastases from a primary gonadal lesion. Sometimes primary gonadal tumors may not be detected on imaging due to tumor regression [47]. Several subtypes of these tumors have been recognized, including seminomas and non-seminomatous GCT (embryonal carcinomas, yolk sac tumors, choriocarcinomas, teratomas, and mixed GCTs).

Retroperitoneal primary SCST arise from ectopically located sex cord stromal tissue or from sex cord-like differentiation of somatic cells. Extragonadal primary SCST are commonly seen in the pelvis, retroperitoneal location is less common. Several types of stromal tumors are recognized, including thecomas, Sertoli–Leydig cell tumors, and unclassified sex cord tumors. Elevated serum estrogen levels are typical in patients with granulosa cell tumors and thecomas.

Imaging findings of SCST are nonspecific: tumors are heterogeneous and enhancing on all cross-sectional imaging modalities. These tumors may demonstrate local invasion (Fig. 10) [48–50].

Teratoma Retroperitoneal teratomas represent 10% of all teratomas and originate from ectopically located pluripotent germ cells [51, 52]. Teratomas are subdivided into three main categories: mature (cystic/solid, most are benign), immature (malignant) and monodermal (highly differentiated) [53]. Imaging may not reliably differentiate these types.

Mature teratomas (also called dermoid cysts) are predominately cystic. Calcifications and fat components are common. The large cystic components contain fatty sebaceous fluid and fat-fluid or fluid-fluid levels. Malignant transformation occurs in 2–3% of mature teratomas, specifically adenocarcinoma type [7].

Immature teratomas consist of 10% of undifferentiated tissue [50]. Elevated AFP levels may be present. On CT and MRI they appear as enhancing predominantly solid masses of variable CT attenuation and MR signal, with foci of fat, calcification, and simple cysts (Video 4). Local and vascular invasion is partly responsible for their poor prognosis. Treatment is surgical [5].

Primary non-neoplastic retroperitoneal conditions Multiple non-neoplastic disease entities may be encountered in the retroperitoneum (Table 2), with more common entities including abscess, arteriovenous malformations (AVM), and hematoma, and less common ones including amyloidosis, retroperitoneal fibrosis, Erdheim–Chester disease, extramedullary hematopoiesis, and Castleman disease.

Retroperitoneal hemorrhage and AVM are the most common vascular lesions of the retroperitoneum. Ill-defined, infiltrative morphology, and high attenuation on unenhanced CT distinguish hemorrhage from neoplasms (Fig. 11). A blush of enhancement may be present from extravasation if there is active hemorrhage. AVM present as a tangle of enlarged vessels on CT and MRI, with prominent flow voids on T2WI. Further characteristics of these entities are listed in Table 2.

Retroperitoneal fibrosis and Erdheim–Chester disease Retroperitoneal fibrosis (RPF) and Erdheim–Chester disease

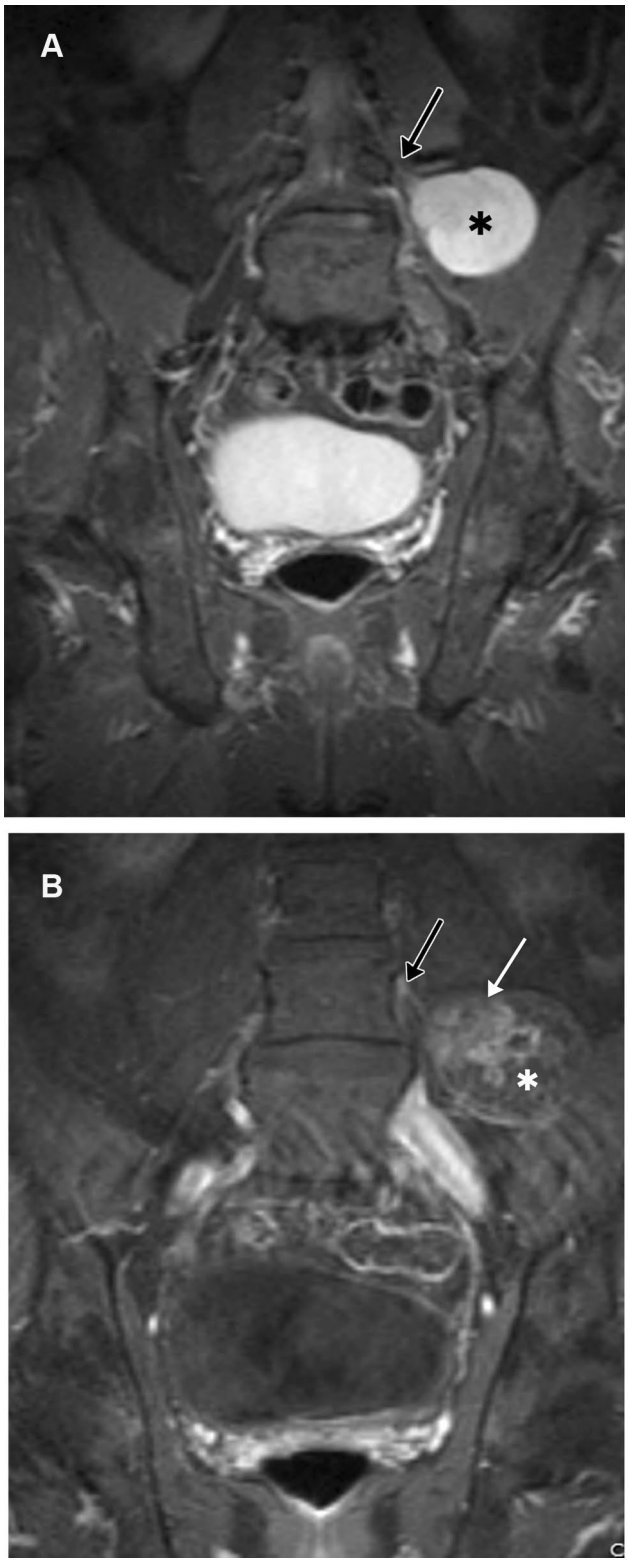

Fig. 7 A. Schwannoma in a 52-year-old male. **a** Coronal Fat Sat ▶ T2-weighted image of the pelvis demonstrating T2 hyperintense mass to left of the L4–L5 disk space (asterisk). **b** Coronal T1W FS post-contrast image showing heterogeneous enhancement (white arrow) of the mass (asterisk). An L4–L5 nerve appears to be entering the mass (black arrows in **a**, **b**). The mass is associated with the left L4–L5 neural foramina. **b** Schwannoma in a 52-year-old male. **a** Coronal Fat Sat T2-weighted image of the pelvis demonstrating T2 hyperintense mass to left of the L4–L5 disk space (asterisk). **b** Coronal T1W FS post-contrast image showing heterogeneous enhancement (white arrow) of the mass (asterisk). An L4–L5 nerve appears to be entering the mass (black arrows in **a**, **b**). The mass is associated with the left L4–L5 neural foramina

(ECD) may resemble a number of the retroperitoneal neoplasms such as lymphoma, multiple myeloma, metastatic disease and desmoid tumor. Involvement of other systems and organs or pattern of distribution may aid in differentiation of RPF and ECD from malignant processes. Both conditions demonstrate a mantle growth pattern with fibrotic changes encasing the RP structures and vessels and absence of invasion. ECD involves RP visceral organs (especially kidneys and perirenal space), long bones, skin, globes, lungs, brain, pituitary, and heart (Fig. 12). RPF develops around the aortic bifurcation and spreads upward, enveloping renal hila (Fig. 13, Video 5). Both processes may result in ureteral and vascular obstruction [54]. Tethering of vessels to adjacent vertebrae and medial displacement of the ureters are characteristic of nonmalignant RPF. Active inflammation seen in acute stage RPF shows avid enhancement on post-contrast CT and MRI, and T2 hyperintense signal on MRI. Chronic (acellular) RPF demonstrates T2 hypointense signal and delayed or no enhancement on post-contrast imaging. A malignant form of RPF also exists and carries a poor prognosis; it is characterized by large size, irregular lobular margins, variable enhancement, and significant mass effect resulting in anterior displacement of vessels and lateral displacement of the ureters [54].

Extramedullary hematopoiesis The retroperitoneum is an uncommon site for extramedullary hematopoiesis (EMH), which on imaging presents as homogeneous bilateral soft tissue masses that extend along the paravertebral region or arise in the perirenal space, and may contain macroscopic fat, hemosiderin deposits and demonstrate variable enhancement (Fig. 14). Calcifications and bony destruction are rare [55]. Disease processes that affect marrow hematopoiesis result in EMH [7]. The presence of hepatosplenomegaly, anemia and skeletal changes may aid in diagnosis [56, 57].

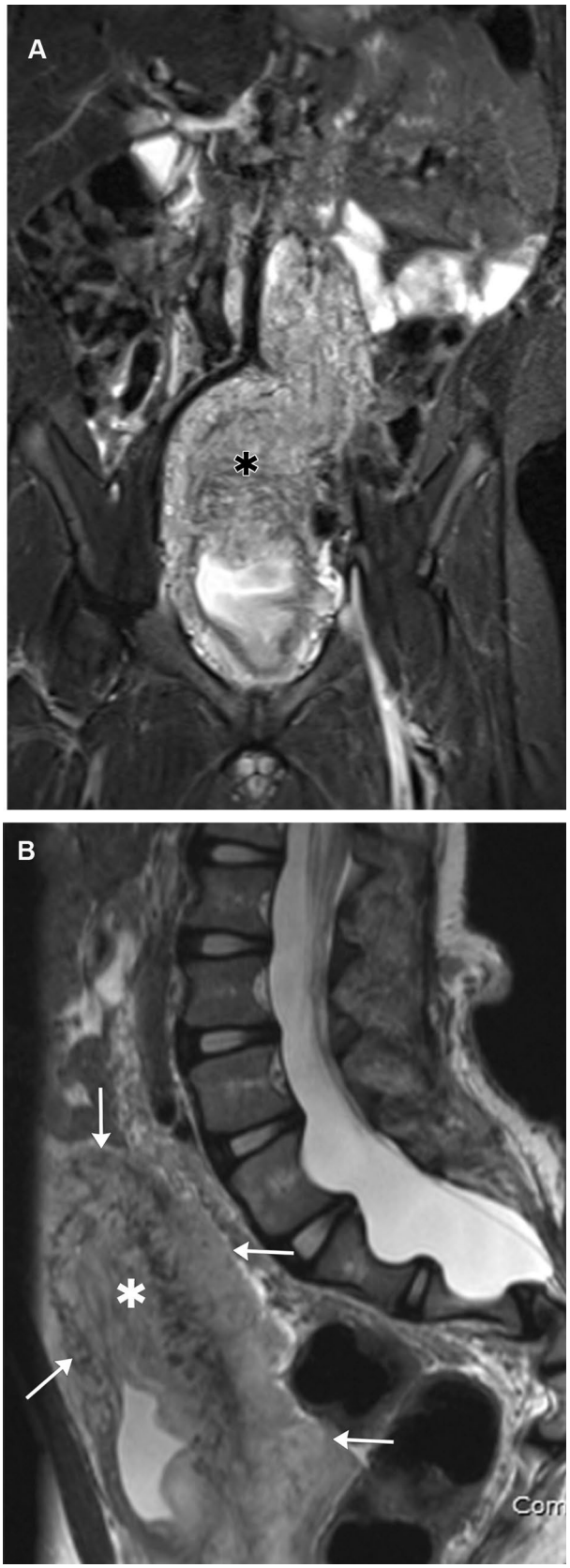

Fig. 8 A Diffuse plexiform neurofibroma in a 23-year-old male with history of Neurofibromatosis Type 1 (NF1). **a** coronal T2W FS and **b** sagittal T2 W TSE image shows an infiltrative mass (asterisk in **a** and arrows and asterisk in **b**) extending along a nerve and surrounding the urinary bladder. Note widening of the thecal sac in this patient with sacral Tarlov's cysts (not shown). **b** Diffuse plexiform neurofibroma in a 23-year-old male with history of Neurofibromatosis Type 1 (NF1). **a** coronal T2W FS and **b** sagittal T2 W TSE image shows an infiltrative mass (asterisk in **a** and arrows and asterisk in **b**) extending along a nerve and surrounding the urinary bladder. Note widening of the thecal sac in this patient with sacral Tarlov's cysts (not shown)

Castleman disease Castleman disease (CD) is a rare disease characterized by the development of benign lymphadenopathy that may be localized or systemic, often mimicking malignancy [58, 59]. On imaging, CD presents as homogeneously hyperenhancing mass(es) some with calcifications (Fig. 15) [60, 61]. Diagnosis requires tissue sampling.

Amyloidosis Amyloidosis is a heterogeneous group of diseases resulting from the extracellular deposition of abnormal protein either at a specific site (localized amyloidosis) or throughout the body (systemic amyloidosis) [62]. It may be a primary disease process or secondary to a variety of chronic infectious, inflammatory, and neoplastic conditions; accordingly, clinical presentation is widely variable. Isolated involvement of the retroperitoneum may occur in localized amyloidosis [63].

CT and MRI features include the replacement of retroperitoneal fat with infiltrative soft tissue representing extracellular deposits of abnormally folded protein, which encases the aorta and retroperitoneal organs (Fig. 16a) and may progressively calcify over time (Fig. 16b). This appearance is similar to RPF and lymphoma, although unlike those conditions amyloid deposits can demonstrate signal dropout on opposed phase T1WI due to the intermixing of lipid and water elements [63]. Protein deposits may coalesce into a discrete mass (amyloidoma) and mimic malignancies including lymphoma or plasmacytoma on cross-sectional imaging. Biopsy is often necessary for diagnosis [63].

Conclusion

Primary retroperitoneal pathologies are a diverse group of benign and malignant conditions that arise within the retroperitoneal space independent of the organs located there. Although the exact diagnosis is often difficult to establish based on imaging alone, a few specific imaging findings on CT and MRI can help in narrowing the differential.

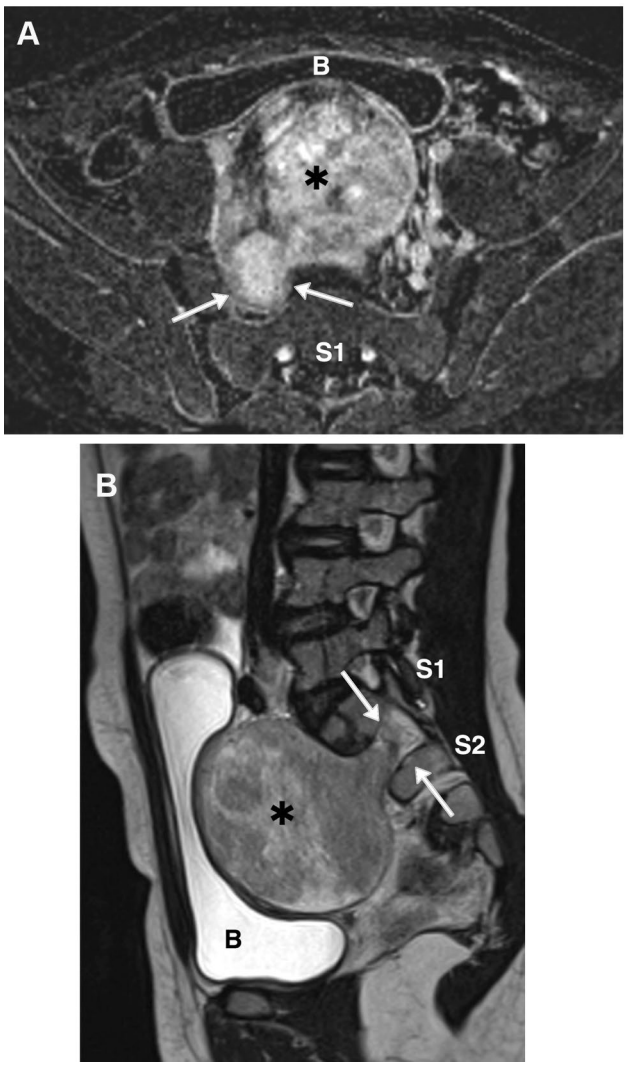

Fig. 9 A Ganglioneuroma in a young female. **b** Axial subtraction T1W FS image demonstrates a large (5×7 cm) heterogeneously enhancing, well -circumscribed pelvic, midline mass (asterisk). The mass extends/arises from the widened right S1-2 neural foramen (arrows). The mass abuts the right ovary and right iliac artery but it does not encase the vasculature and there is no evidence of right ovarian involvement (not shown, B = urinary bladder) **b** Sagittal T2-weighted image reveals heterogeneous hyperintensity signal within the mass. Note mass effect on the adjacent posterior wall of the urinary bladder (**b**). Again appreciated is the extension on the mass into the right S1-2 neural foramen (white arrows). **B** Ganglioneuroma in a young female. **a** Axial subtraction T1W FS image demonstrates a large (5×7 cm) heterogeneously enhancing, well-circumscribed pelvic, midline mass (asterisk). The mass extends/arises from the widened right S1-2 neural foramen (arrows). The mass abuts the right ovary and right iliac artery but it does not encase the vasculature and there is no evidence of right ovarian involvement (not shown, B = urinary bladder) **b**. Sagittal T2-weighted image reveals heterogeneous hyperintense signal within the mass. Note mass effect on the adjacent posterior wall of the urinary bladder (**b**). Again appreciated is the extension on the mass into the right S1-2 neural foramen (white arrows)

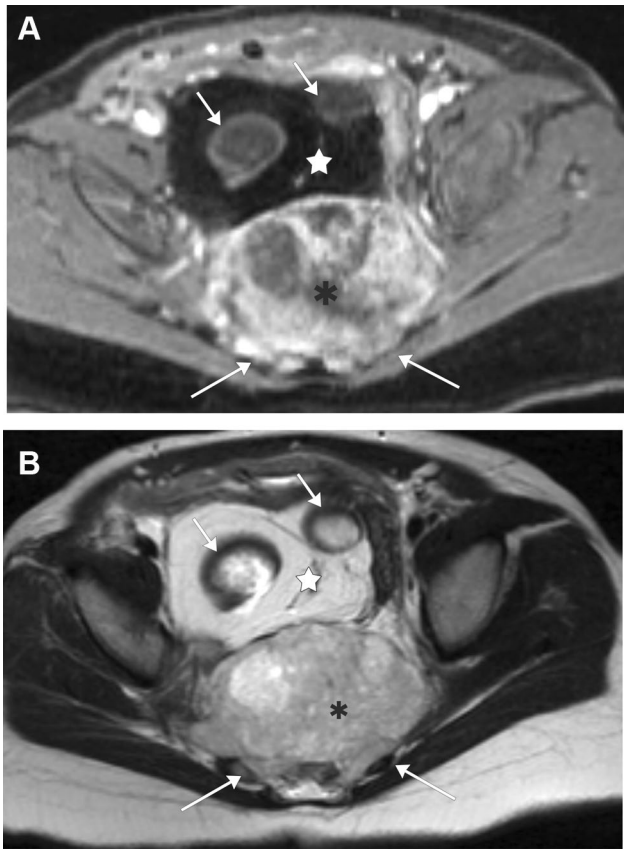

Fig. 10 A Sacrococcygeal Primary Germ Cell Tumor (Yolk Sac type and Mature Teratoma) in a young male patient. **a** Axial T1W FS post-contrast image demonstrates a large 8.5×6 cm heterogeneously enhancing retroperitoneal bilobed mass that is centered within the presacral and precoccygeal space. The mass is composed of two main components: one is more heterogeneously enhancing presacral solid component (asterisk, representing a yolk sac tumor on pathology); and a second more anteriorly positioned minimally to none enhancing fat-containing component (star, representing mature teratoma component of the tumor). **b** Axial T2W TSE image demonstrates heterogeneous T2 signal of the posterior yolk sac component (asterisk) and hyperintense fat (asterisk) and hemorrhage (short white arrows) containing anterior mature teratoma component (star). **b** Sacrococcygeal Primary Germ Cell Tumor (Yolk Sac type and Mature Teratoma) in a young male patient. **a** Axial T1W FS post-contrast image demonstrates a large 8.5×6 cm heterogeneously enhancing retroperitoneal bilobed mass that is centered within the presacral and precoccygeal space. The mass is composed of two main components: one is more heterogeneously enhancing presacral solid component (asterisk, representing a yolk sac tumor on pathology); and a second more anteriorly positioned minimally to none enhancing fat-containing component (star, representing mature teratoma component of the tumor). **b** Axial T2W TSE image demonstrates heterogeneous T2 signal of the posterior yolk sac component (asterisk) and hyperintense fat (asterisk) and hemorrhage (short white arrows) containing anterior mature teratoma component (star)

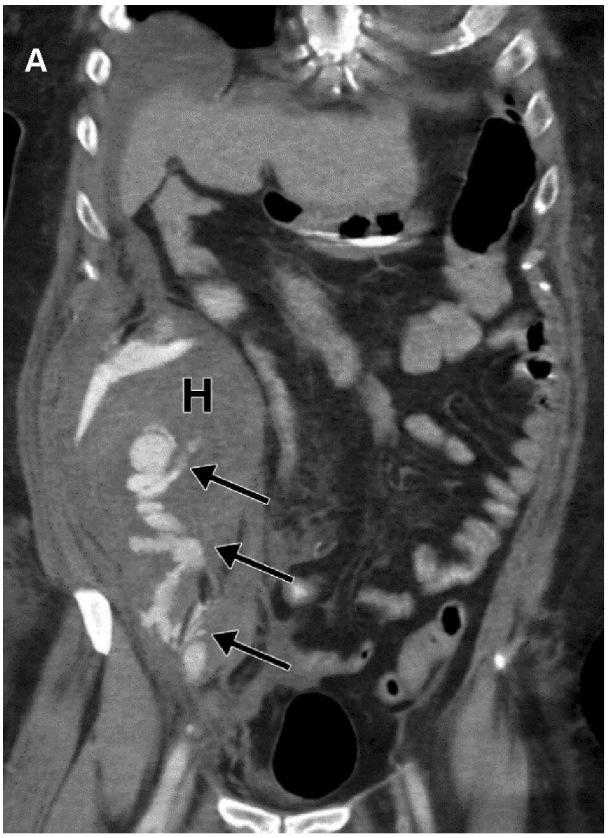

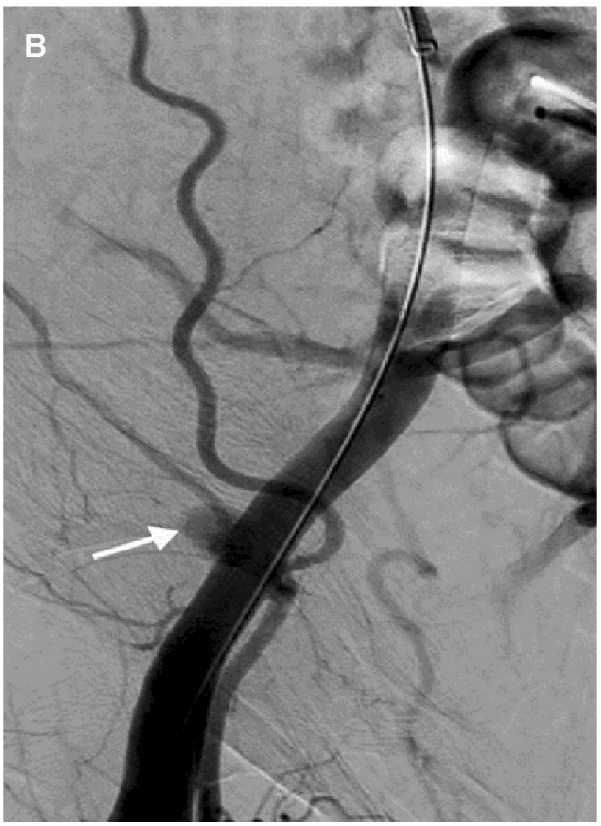

Fig. 11 **a** Retroperitoneal hemorrhage with active extravasation from a ruptured pseudoaneurysm (PSA) in a 52-year-old female status post catheter directed spasmolysis one day ago. **a** IV contrast-enhanced CT image obtained in the coronal plane demonstrates a large right retroperitoneal hemorrhage (H) with an active extravasation (black arrows in **a**). **b** Selective arteriogram of the common iliac artery demonstrates a small pseudoaneurysm of the right distal external iliac artery (R EIA) (arrow in **b**). Active extravasation was noted on dynamic imaging (not shown). The patient underwent successful thrombin injection of the PSA. **b** Retroperitoneal hemorrhage with active extravasation from a ruptured pseudoaneurysm (PSA) in a 52-year-old female status post catheter directed spasmolysis one day ago. **a** IV contrast-enhanced CT image obtained in the coronal plane demonstrates a large right retroperitoneal hemorrhage (H) with an active extravasation (black arrows in **a**). **b** Selective arteriogram of the common iliac artery demonstrates a small pseudoaneurysm of the right distal external iliac artery (R EIA) (arrow in **b**). Active extravasation was noted on dynamic imaging (not shown) The patient underwent successful thrombin injection of the PSA

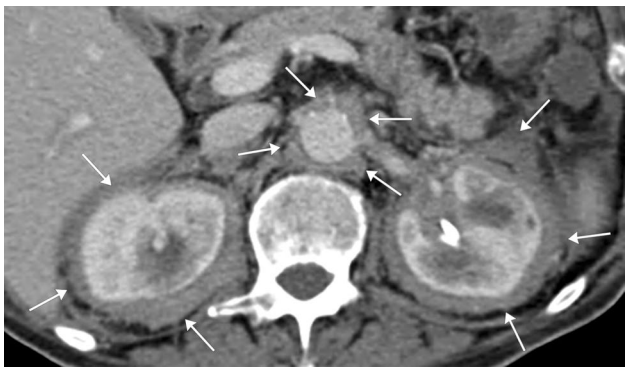

Fig. 12 Erdheim–Chester disease in a middle-aged male. Axial post-contrast CT image obtained at the level of the kidneys shows bilateral perirenal and periaortic soft tissue encasement (arrows)

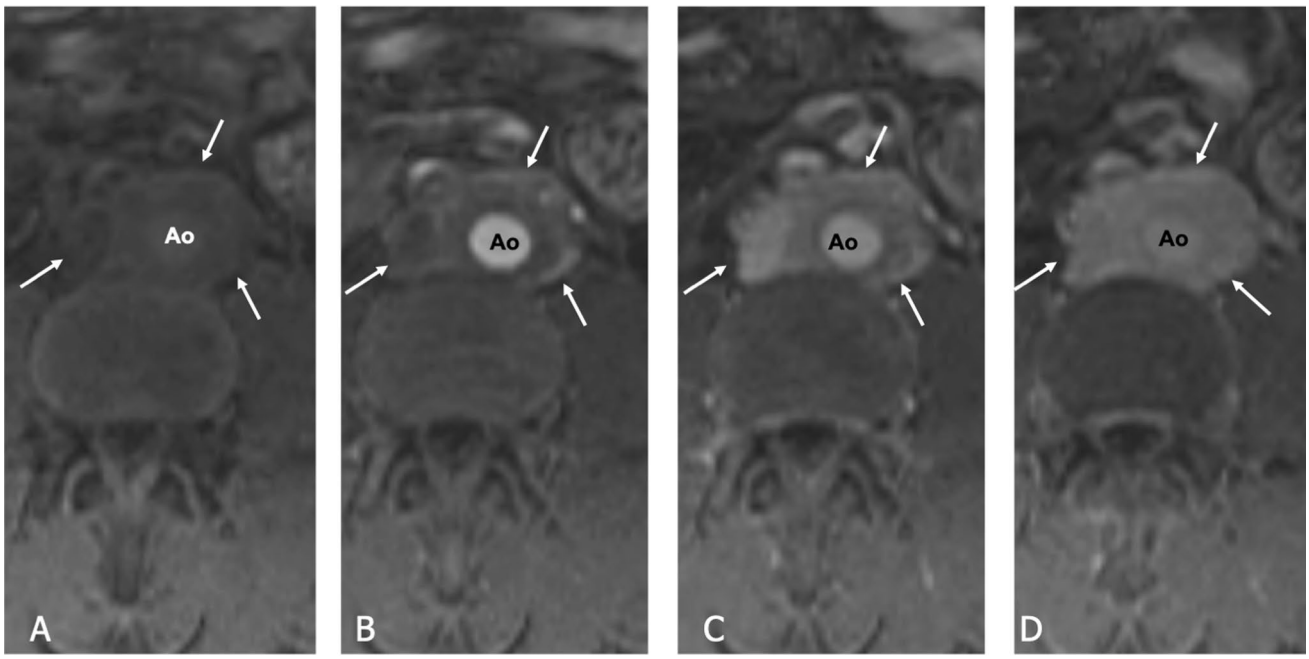

Fig. 13 Retroperitoneal fibrosis in a middle-aged woman. Pre-contrast (**a**) and dynamic post-contrast (**b**–**d**) T1W FS images show infiltrating soft tissue in the retroperitoneum (arrows) encasing the aorta (Ao). Progressive enhancement most pronounced on the delayed phase (**d**) indicates active inflammation

Fig. 14 Extramedullary hematopoiesis. Contrast-enhanced CT at the level of the kidneys shows bilateral mixed fat and soft tissue attenuation masses (arrows) representing hematopoetic tissue in the anterior pararenal and perirenal space in a patient with profound, chronic anemia. Although the masses are heterogeneous, calcifications and fluid density components are absent. RK = right kidney, LK = left kidney

Fig. 15 Castleman's disease in a middle-aged male. Axial contrast-enhanced CT shows an avidly enhancing retroperitoneal soft tissue mass (M) near the left iliac vessels exerting mass effect on the left psoas muscle. Soft tissue attenuation (asterisk) around the mass representing lymphoid tissue infiltrates the retroperitoneal fat around the mass

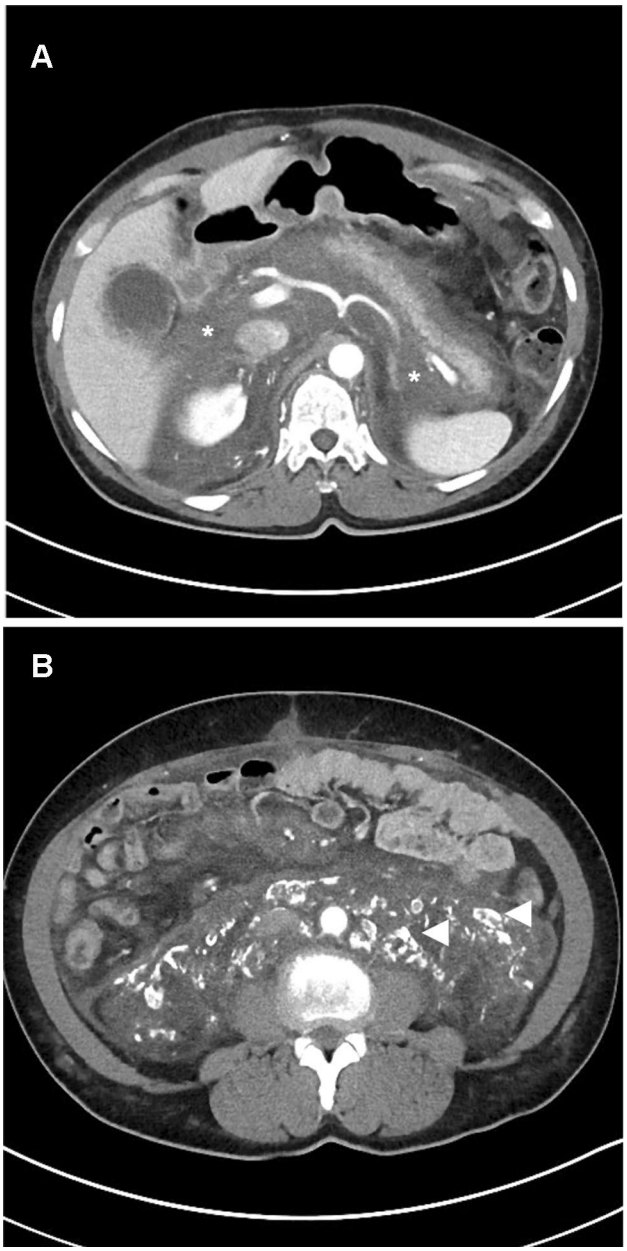

Fig. 16 **a** Retroperitoneal amyloidosis in a 64-year-old man. **a** Axial contrast-enhanced CT of the abdomen shows infiltrative soft tissue surrounding the aorta and replacing retroperitoneal fat (asterisk). **b** Axial contrast\-enhanced CT shows several coarse calcifications, usually seen in chronic amyloid deposits, throughout the infiltrative soft tissue (arrowheads). **b** Retroperitoneal amyloidosis in a 64-year-old man. **a** Axial contrast-enhanced CT of the abdomen shows infiltrative soft tissue surrounding the aorta and replacing retroperitoneal fat (asterisk). **b** Axial contrast-enhanced CT shows several coarse calcifications, usually seen in chronic amyloid deposits, throughout the infiltrative soft tissue (arrowheads)

Familiarity with the epidemiology, pathogenesis, imaging features, and treatment of these retroperitoneal entities can aid radiologic diagnoses and guide appropriate patient management.

Electronic supplementary material The online version of this article (https://doi.org/10.1007/s00261-020-02752-8) contains supplementary material, which is available to authorized users.

Acknowledgements The authors thank Henry Douglas for his help with images.

Compliance with ethical standards

Conflict of interest The authors declare that they have no conflicts of interest.

Ethical approval This article does not contain any studies with animals performed by any of the authors. All procedures performed in studies involving human participants were in accordance with the ethical standards of the institutional and/or national research committee and with the 1964 Helsinki declaration and its later amendments or comparable ethical standards.

References

1. Mota M, Bezerra ROF, Garcia MRT (2018) Practical approach to primary retroperitoneal masses in adults. Radiol Bras 51 (6):391-400. https://doi.org/10.1590/0100-3984.2017.0179
2. Goenka AH, Shah SN, Remer EM (2012) Imaging of the retroperitoneum. Radiol Clin North Am 50 (2):333-355, vii. https://doi.org/10.1016/j.rcl.2012.02.004
3. Elsayes KM, Staveteig PT, Narra VR, Chen ZM, Moustafa YL, Brown J (2007) Retroperitoneal masses: magnetic resonance imaging findings with pathologic correlation. Curr Probl Diagn Radiol 36 (3):97-106. https://doi.org/10.1067/j.cpradiol.2006.12.003
4. Scali EP, Chandler TM, Heffernan EJ, Coyle J, Harris AC, Chang SD (2015) Primary retroperitoneal masses: what is the differential diagnosis? Abdom Imaging 40 (6):1887-1903. https://doi.org/10.1007/s00261-014-0311-x
5. Rajiah P, Sinha R, Cuevas C, Dubinsky TJ, Bush WH, Jr., Kolokythas O (2011) Imaging of uncommon retroperitoneal masses. Radiographics 31 (4):949-976. https://doi.org/10.1148/rg.314095132
6. Nishino M, Hayakawa K, Minami M, Yamamoto A, Ueda H, Takasu K (2003) Primary retroperitoneal neoplasms: CT and MR imaging findings with anatomic and pathologic diagnostic clues. Radiographics 23 (1):45-57. https://doi.org/10.1148/rg.231025037
7. Shaaban AM, Rezvani M, Tubay M, Elsayes KM, Woodward PJ, Menias CO (2016) Fat-containing Retroperitoneal Lesions: Imaging Characteristics, Localization, and Differential Diagnosis. Radiographics 36 (3):710-734. https://doi.org/10.1148/rg.2016150149
8. Craig WD, Fanburg-Smith JC, Henry LR, Guerrero R, Barton JH (2009) Fat-containing lesions of the retroperitoneum: radiologic-pathologic correlation. Radiographics 29 (1):261-290. https://doi.org/10.1148/rg.291085203
9. Jagannathan JP, Tirumani SH, Ramaiya NH (2016) Imaging in Soft Tissue Sarcomas: Current Updates. Surg Oncol Clin N Am 25 (4):645-675. https://doi.org/10.1016/j.soc.2016.05.002

10. Elnemr A, Yonemura Y, Shinbo M, Nishino E (2010) Primary retroperitoneal mullerian adenocarcinoma. Rare Tumors 2 (1):e6. https://doi.org/10.4081/rt.2010.e6
11. Weiss SW (1996) Lipomatous tumors. Monogr Pathol 38:207-239
12. Fiore M, Grosso F, Lo Vullo S, Pennacchioli E, Stacchiotti S, Ferrari A, Collini P, Lozza L, Mariani L, Casali PG, Gronchi A (2007) Myxoid/round cell and pleomorphic liposarcomas: prognostic factors and survival in a series of patients treated at a single institution. Cancer 109 (12):2522-2531. https://doi.org/10.1002/cncr.22720
13. Hekimoglu K (2013) Giant retroperitoneal liposarcomas: diagnostic approach with multidetector computed tomography and magnetic resonance imaging. Jbr-Btr 96 (6):375-377. https://doi.org/10.5334/jbr-btr.466
14. Ghadimi MP, Al-Zaid T, Madewell J, Peng T, Colombo C, Hoffman A, Creighton CJ, Zhang Y, Zhang A, Lazar AJ, Pollock RE, Lev D (2011) Diagnosis, management, and outcome of patients with dedifferentiated liposarcoma systemic metastasis. Ann Surg Oncol 18 (13):3762-3770. https://doi.org/10.1245/s10434-011-1794-0
15. Baheti AD, O'Malley RB, Kim S, Keraliya AR, Tirumani SH, Ramaiya NH, Wang CL (2016) Soft-Tissue Sarcomas: An Update for Radiologists Based on the Revised 2013 World Health Organization Classification. AJR Am J Roentgenol 206 (5):924-932. https://doi.org/10.2214/AJR.15.15498
16. Levy AD, Manning MA, Al-Refaie WB, Miettinen MM (2017) Soft-Tissue Sarcomas of the Abdomen and Pelvis: Radiologic-Pathologic Features, Part 1-Common Sarcomas: From the Radiologic Pathology Archives. Radiographics 37 (2):462-483. https://doi.org/10.1148/rg.2017160157
17. Lahat G, Madewell JE, Anaya DA, Qiao W, Tuvin D, Benjamin RS, Lev DC, Pollock RE (2009) Computed tomography scan-driven selection of treatment for retroperitoneal liposarcoma histologic subtypes. Cancer 115 (5):1081-1090. https://doi.org/10.1002/cncr.24045
18. Kim EY, Kim SJ, Choi D, Lee SJ, Kim SH, Lim HK, Song SY (2008) Recurrence of retroperitoneal liposarcoma: imaging findings and growth rates at follow-up CT. AJR Am J Roentgenol 191 (6):1841-1846. https://doi.org/10.2214/AJR.07.3746
19. Kim T, Murakami T, Oi H, Tsuda K, Matsushita M, Tomoda K, Fukuda H, Nakamura H (1996) CT and MR imaging of abdominal liposarcoma. AJR Am J Roentgenol 166 (4):829-833. https://doi.org/10.2214/ajr.166.4.8610559
20. Hong SH, Kim KA, Woo OH, Park CM, Kim CH, Kim MJ, Chung JJ, Han JK, Rha SE (2010) Dedifferentiated liposarcoma of retroperitoneum: spectrum of imaging findings in 15 patients. Clin Imaging 34 (3):203-210. https://doi.org/10.1016/j.clinimag.2009.12.025
21. Cooley CL, Jagannathan JP, Kurra V, Tirumani SH, Saboo SS, Ramaiya NH, Shinagare AB (2014) Imaging features and metastatic pattern of non-IVC retroperitoneal leiomyosarcomas: are they different from IVC leiomyosarcomas? J Comput Assist Tomogr 38 (5):687-692. https://doi.org/10.1097/RCT.0000000000000097
22. Abraham JA, Weaver MJ, Hornick JL, Zurakowski D, Ready JE (2012) Outcomes and prognostic factors for a consecutive case series of 115 patients with somatic leiomyosarcoma. J Bone Joint Surg Am 94 (8):736-744. https://doi.org/10.2106/JBJS.K.00460
23. Ganeshalingam S, Rajeswaran G, Jones RL, Thway K, Moskovic E (2011) Leiomyosarcomas of the inferior vena cava: diagnostic features on cross-sectional imaging. Clin Radiol 66 (1):50-56. https://doi.org/10.1016/j.crad.2010.08.004
24. O'Sullivan PJ, Harris AC, Munk PL (2008) Radiological imaging features of non-uterine leiomyosarcoma. Br J Radiol 81 (961):73-81. https://doi.org/10.1259/bjr/18595145
25. Yakupoglu A, Ulus S, Cantasdemir M (2016) Leiomyosarcoma of the Inferior Vena Cava Confirmed by Aspiration Biopsy With a Catheter During Digital Subtraction Angiography. Vasc Endovascular Surg 50 (3):164-167. https://doi.org/10.1177/1538574416637445
26. Huang J, Liu Q, Lu JP, Wang F, Wang L, Jin AG (2011) Primary intraluminal leiomyosarcoma of the inferior vena cava: value of MRI with contrast-enhanced MR venography in diagnosis and treatment. Abdom Imaging 36 (3):337-341. https://doi.org/10.1007/s00261-010-9656-y
27. Brennan MF, Antonescu CR, Alektiar KM, Maki RG (2016) Undifferentiated Pleomorphic Sarcoma (UPS) (Malignant Fibrous Histiocytoma (MFH) and Myxofibrosarcoma). In: Management of Soft Tissue Sarcoma. Springer International Publishing, Cham, pp 143-152. https://doi.org/10.1007/978-3-319-41906-0_7
28. Cong Z, Gong J (2011) Primary malignant fibrous histiocytoma of the liver: CT findings in five histopathological proven patients. Abdom Imaging 36 (5):552-556. https://doi.org/10.1007/s00261-011-9691-3
29. Osman S, Lehnert BE, Elojeimy S, Cruite I, Mannelli L, Bhargava P, Moshiri M (2013) A comprehensive review of the retroperitoneal anatomy, neoplasms, and pattern of disease spread. Curr Probl Diagn Radiol 42 (5):191-208. https://doi.org/10.1067/j.cpradiol.2013.02.001
30. Kim KH, Lee SH, Cha SH, Kim YS, Sung DJ (2012) Malignant fibrous histiocytoma arising from a hydronephrotic kidney: a case report and review of the literature. Clin Imaging 36 (3):239-242. https://doi.org/10.1016/j.clinimag.2011.09.001
31. Lee SY, Jee WH, Jung JY, Park MY, Kim SK, Jung CK, Chung YG (2016) Differentiation of malignant from benign soft tissue tumours: use of additive qualitative and quantitative diffusion-weighted MR imaging to standard MR imaging at 3.0 T. Eur Radiol 26 (3):743-754. https://doi.org/10.1007/s00330-015-3878-x
32. Gaballah AH, Jensen CT, Palmquist S, Pickhardt PJ, Duran A, Broering G, Elsayes KM (2017) Angiosarcoma: clinical and imaging features from head to toe. Br J Radiol 90 (1075):20170039. https://doi.org/10.1259/bjr.20170039
33. Sung CK, Kim B, Moon KC, Ku JH, Ha SB (2017) Retroperitoneal Tumors. In: Kim SH, Cho JY (eds) Oncologic Imaging: Urology. Springer Berlin Heidelberg, Berlin, Heidelberg, pp 227-260. https://doi.org/10.1007/978-3-662-45218-9_6
34. Miao C, Luo C-H (2018) Retroperitoneal Rhabdomyosarcoma. In: Luo C-H (ed) Retroperitoneal Tumors. Springer Netherlands, Dordrecht, pp 183-184. https://doi.org/10.1007/978-94-024-1167-6_17
35. Miao C, Luo C-H (2018) Retroperitoneal Synovial Sarcoma. In: Luo C-H (ed) Retroperitoneal Tumors. Springer Netherlands, Dordrecht, pp 259-261. https://doi.org/10.1007/978-94-024-1167-6_33
36. Thway K, Fisher C (2015) PEComa: morphology and genetics of a complex tumor family. Ann Diagn Pathol 19 (5):359-368. https://doi.org/10.1016/j.anndiagpath.2015.06.003
37. Crino PB, Nathanson KL, Henske EP (2006) The tuberous sclerosis complex. N Engl J Med 355 (13):1345-1356. https://doi.org/10.1056/NEJMra055323
38. Phillips CH, Keraliya AR, Shinagare AB, Ramaiya NH, Tirumani SH (2016) Update on the imaging of malignant perivascular epithelioid cell tumors (PEComas). Abdom Radiol (NY) 41 (2):368-376. https://doi.org/10.1007/s00261-015-0568-8
39. Liang W, Xu C, Chen F (2015) Primary retroperitoneal perivascular epithelioid cell neoplasm: A case report. Oncol Lett 10 (1):469-472. https://doi.org/10.3892/ol.2015.3210
40. Hedgire SS, Kudrimoti S, Oliveira IS, Nadkarni N, McDermott S, Hahn PF, Mino-Kenudson M, Harisinghani MG (2017) Extranodal lymphomas of abdomen and pelvis: imaging findings and

differential diagnosis. Abdom Radiol (NY) 42 (4):1096-1112. https://doi.org/10.1007/s00261-016-0964-8
41. Rosenkrantz AB, Spieler B, Seuss CR, Stifelman MD, Kim S (2012) Utility of MRI features for differentiation of retroperitoneal fibrosis and lymphoma. AJR Am J Roentgenol 199 (1):118-126. https://doi.org/10.2214/AJR.11.7822
42. Neville A, Herts BR (2004) CT characteristics of primary retroperitoneal neoplasms. Crit Rev Comput Tomogr 45 (4):247-270
43. Rha SE, Byun JY, Jung SE, Chun HJ, Lee HG, Lee JM (2003) Neurogenic tumors in the abdomen: tumor types and imaging characteristics. Radiographics 23 (1):29-43. https://doi.org/10.1148/rg.231025050
44. MJ, Thomas JM, Fisher C, Moskovic EC (2005) Imaging features of retroperitoneal and pelvic schwannomas. Clin Radiol 60 (8):886-893. https://doi.org/10.1016/j.crad.2005.01.016
45. Erickson D, Kudva YC, Ebersold MJ, Thompson GB, Grant CS, van Heerden JA, Young WF, Jr. (2001) Benign paragangliomas: clinical presentation and treatment outcomes in 236 patients. J Clin Endocrinol Metab 86 (11):5210-5216. https://doi.org/10.1210/jcem.86.11.8034
46. Lonergan GJ, Schwab CM, Suarez ES, Carlson CL (2002) Neuroblastoma, ganglioneuroblastoma, and ganglioneuroma: radiologic-pathologic correlation. Radiographics 22 (4):911-934. https://doi.org/10.1148/radiographics.22.4.g02jl15911
47. Choyke PL, Hayes WS, Sesterhenn IA (1993) Primary extragonadal germ cell tumors of the retroperitoneum: differentiation of primary and secondary tumors. Radiographics 13 (6):1365-1375; quiz 1377-1368. https://doi.org/10.1148/radiographics.13.6.8290730
48. Keitoku M, Konishi I, Nanbu K, Yamamoto S, Mandai M, Kataoka N, Oishi T, Mori T (1997) Extraovarian sex cord-stromal tumor: case report and review of the literature. Int J Gynecol Pathol 16 (2):180-185. https://doi.org/10.1097/00004347-199704000-00017
49. Trabelsi A, Ben Abdelkarim S, Hadfi M, Fatnaci R, Stita W, Sriha B, Korbi S (2008) Primary mesenteric Sertoli–Leydig cell tumor: a case report and review of the literature. J Oncol 2008:619637. https://doi.org/10.1155/2008/619637
50. Ueno T, Tanaka YO, Nagata M, Tsunoda H, Anno I, Ishikawa S, Kawai K, Itai Y (2004) Spectrum of germ cell tumors: from head to toe. Radiographics 24 (2):387-404. https://doi.org/10.1148/rg.242035082
51. Gatcombe HG, Assikis V, Kooby D, Johnstone PA (2004) Primary retroperitoneal teratomas: a review of the literature. J Surg Oncol 86 (2):107-113. https://doi.org/10.1002/jso.20043
52. Davidson AJ, Hartman DS, Goldman SM (1989) Mature teratoma of the retroperitoneum: radiologic, pathologic, and clinical correlation. Radiology 172 (2):421-425. https://doi.org/10.1148/radiology.172.2.2664866
53. Mathur P, Lopez-Viego MA, Howell M (2010) Giant primary retroperitoneal teratoma in an adult: a case report. Case Rep Med 2010. https://doi.org/10.1155/2010/650424
54. Surabhi VR, Menias C, Prasad SR, Patel AH, Nagar A, Dalrymple NC (2008) Neoplastic and non-neoplastic proliferative disorders of the perirenal space: cross-sectional imaging findings. Radiographics 28 (4):1005-1017. https://doi.org/10.1148/rg.28407515
55. Mesurolle B, Sayag E, Meingan P, Lasser P, Duvillard P, Vanel D (1996) Retroperitoneal extramedullary hematopoiesis: sonographic, CT, and MR imaging appearance. AJR Am J Roentgenol 167 (5):1139-1140. https://doi.org/10.2214/ajr.167.5.8911166
56. Georgiades CS, Neyman EG, Francis IR, Sneider MB, Fishman EK (2002) Typical and atypical presentations of extramedullary hemopoiesis. AJR Am J Roentgenol 179 (5):1239-1243. https://doi.org/10.2214/ajr.179.5.1791239
57. Orphanidou-Vlachou E, Tziakouri-Shiakalli C, Georgiades CS (2014) Extramedullary hemopoiesis. Semin Ultrasound CT MR 35 (3):255-262. https://doi.org/10.1053/j.sult.2013.12.001
58. Zhou LP, Zhang B, Peng WJ, Yang WT, Guan YB, Zhou KR (2008) Imaging findings of Castleman disease of the abdomen and pelvis. Abdom Imaging 33 (4):482-488. https://doi.org/10.1007/s00261-007-9282-5
59. Cohn JE, Zhou J, Hu A (2018) Castleman disease. Ear Nose Throat J 97 (8):233-234. https://doi.org/10.1177/014556131809700819
60. Meador TL, McLarney JK (2000) CT features of Castleman disease of the abdomen and pelvis. AJR Am J Roentgenol 175 (1):115-118. https://doi.org/10.2214/ajr.175.1.1750115
61. Irsutti M, Paul JL, Selves J, Railhac JJ (1999) Castleman disease: CT and MR imaging features of a retroperitoneal location in association with paraneoplastic pemphigus. Eur Radiol 9 (6):1219-1221. https://doi.org/10.1007/s003300050821
62. Czeyda-Pommersheim F, Hwang M, Chen SS, Strollo D, Fuhrman C, Bhalla S (2015) Amyloidosis: Modern Cross-sectional Imaging. Radiographics 35 (5):1381-1392. https://doi.org/10.1148/rg.2015140179
63. Kawashima A, Alleman WG, Takahashi N, Kim B, King BF, Jr., LeRoy AJ (2011) Imaging evaluation of amyloidosis of the urinary tract and retroperitoneum. Radiographics 31 (6):1569-1582. https://doi.org/10.1148/rg.316115519

Publisher's Note Springer Nature remains neutral with regard to jurisdictional claims in published maps and institutional affiliations.